Structural Dependence of Quadrupole Coupling Constant e^2qQ/h for ^{27}Al and Crystal Field Parameter D for Fe^{3+} in Aluminosilicates

Subrata Ghose

*Department of Geological Sciences, University of Washington,
Seattle, Washington 98195*

Tung Tsang

Department of Physics, Howard University, Washington, D.C. 20001

Abstract

The ^{27}Al nuclear quadrupole coupling tensors and the Fe^{3+} paramagnetic resonance fine-structure constants in minerals have been compared with the geometries of oxygen coordination polyhedra. The nuclear quadrupole coupling constant seems to depend on Al–O bond length variations for octahedrally coordinated sites. However, for tetrahedrally coordinated sites, the coupling constant depends mostly on O–Al–O bond angle variations and only slightly on variations of Al–O bond length. The correlation between NMR and EPR data is poor; the nearest neighbor oxygen coordinations around Al and around Fe may be somewhat different.

Introduction

Modern spectroscopic techniques, such as nuclear magnetic resonance (NMR), electron paramagnetic resonance (EPR), Mössbauer effect, and optical spectra, are now important branches of solid state science and have considerably influenced the electronic and structural theories of crystals. Both the experimental results and the basic theories have been reviewed by Cohen and Reif (1957) for NMR and by Abragam and Bleaney (1970) for EPR. The applications of magnetic resonance techniques to mineralogy have also been very fruitful. Since Al^{3+} and Fe^{3+} ions are important constituents of minerals, the ^{27}Al NMR and the Fe^{3+} EPR spectra have been extensively studied. From the experimental data, the Fe^{3+} fine structure and the ^{27}Al nuclear quadrupole coupling tensors may be obtained. These tensors are related to the deviations of the local site symmetries from perfect octahedral or tetrahedral coordinations in the crystal structure. Therefore these tensors are very sensitive parameters of the actual electron density distribution due to chemical bonding and due to the net charges of the neighboring atoms.

In recent years, as a result of the crystal structure refinements by X-ray and neutron diffraction methods, the atomic parameters are now accurately known for many mineral structures. In this paper, attempts will be made to correlate the ^{27}Al NMR and the Fe^{3+} EPR data with the structural distortions for both octahedrally and tetrahedrally coordinated sites in aluminosilicates. Such correlations may be useful in the site assignment of the NMR and EPR spectra in structures where the Al-sites do not possess any point group symmetry (*e.g.,* anorthite, $CaAl_2Si_2O_8$).

Nuclear Magnetic Resonance

Consider a nucleus with spin I, magnetic dipole moment $\vec{\mu} = \gamma h \vec{I}$. For $I \geq 1$, the nucleus may also have electric quadrupole moment eQ. When a crystal is placed in an external constant magnetic field $\vec{H}_0$, the total Hamiltonian (or the total interaction) $\mathcal{H}$ of the nucleus is given by (Cohen and Reif, 1957):

$$\mathcal{H} = \mathcal{H}_Z + \mathcal{H}_Q \tag{1}$$

where the Zeeman Hamiltonian $\mathcal{H}_Z$ is the interaction of the magnetic dipole moment of the nucleus with the external magnetic field $\vec{H}_0$,

$$\mathcal{H}_Z = -\vec{\mu} \cdot \vec{H}_0 = -\gamma h \vec{I} \cdot \vec{H}_0. \tag{2}$$

An electric field gradient arises from a non-octahedral or non-tetrahedral external charge distribution. Following the standard notations of Cohen and Reif (1957), the field gradient tensor components are designated as $-V_{xx}, -V_{yy}, -V_{zz} = -eq$ in

the principal axes (x, y, z) system, with $V_{xx} + V_{yy} + V_{zz} = 0$, $|V_{zz}| \geq |V_{yy}| \geq |V_{xx}|$ and $V_{xy} = V_{yz} = V_{zx} = 0$. The quadrupole Hamiltonian $\mathcal{H}_Q$ is the interaction of the nuclear electric quadrupole moment eQ with this field gradient:

$$\mathcal{H}_Q = \frac{eQ V_{zz}}{4I(2I-1)} [(3I_z^2 - I^2) + \eta(I_x^2 - I_y^2)] \quad (3)$$

This interaction is characterized by the quadrupole coupling constant $C = |e^2qQ/h|$, the asymmetry parameter $\eta = (V_{xx} - V_{yy})/V_{zz}$ and the directions of the principal axes. The coupling constant C, usually expressed in MHz, is a measure of the maximum distortion of the coordination polyhedra. The dimensionless asymmetry parameter η $(0 \leq \eta \leq 1)$ is a measure of deviation from axial symmetry. For example, Al atoms are located on threefold axes in corundum, thus the site symmetry requires $\eta = 0$.

If $\mathcal{H}_Q = 0$, then there will be $2I + 1$ equally spaced energy levels,

$$E = -\gamma H_0 \hbar I, -\gamma H_0 \hbar(I-1), \cdots -\gamma H_0 \hbar I$$

Since resonance occurs when the radio-frequency photon energy matches the energy difference between adjacent levels, a single NMR line would be observed. For ^{27}Al NMR in minerals, usually we have $\mathcal{H}_Q \ll \mathcal{H}_Z$. The quadrupole interaction $\mathcal{H}_Q$ causes different shifts for different energy levels, hence the NMR line is now split into $2I$ components. From the NMR line positions for various relative orientations between the crystal and the external magnetic field $\vec{H}_0$, the quadrupole coupling constant, C, asymmetry parameter η and the orientations of the principal axes may be obtained using standard procedures (Cohen and Reif, 1957).

Electron Paramagnetic Resonance

In Russell-Saunders coupling, the ground state of Fe^{3+} is $^6S_{5/2}$, with total spin angular momentum $S = \frac{5}{2}$ and total orbital angular momentum $L = 0$. For the free Fe^{3+} ion in the presence of an external magnetic field, there will be $2S + 1 = 6$ equally spaced Zeeman energy levels because of the Zeeman interaction (Abragam and Bleaney, 1970).

$$\mathcal{H}_Z = g\beta\vec{H}_0 \cdot \vec{S} \quad (4)$$

where β is the Bohr magneton, and g is very close to the free electron value 2.002. Since the Zeeman energy levels are equally spaced, one EPR line will be observed, very close to the free electron case. The ^{57}Fe hyperfine splittings are very small and may be neglected.

In crystal environment with non-octahedral or non-tetrahedral symmetry, there will be further splittings due to crystal electric field effects, known as fine structures. The total interaction (with both external $\vec{H}_0$ and crystal field) for Fe^{3+} may be represented by a spin Hamiltonian; in the principal axes system (Abragam and Bleaney, 1970; Low and Offenbacher, 1965), we have

$$\mathcal{H} = g\beta\vec{H} \cdot \vec{S} + D[S_z^2 - 1/3\, S\,(S+1)]$$
$$+ E[S_x^2 - S_y^2] + \cdots \quad (5)$$

where the first term is the Zeeman interaction. The other terms describe the fine structure due to crystal electric field effects. The higher order terms of the spin Hamiltonian, with terms such as S^4, are usually small and may be neglected. The principal axes system are usually chosen such that $0 < 3E/D < 1$.

Distortion of the Coordination Polyhedra

The nuclear quadrupole coupling constant C, the asymmetry parameter η and the principal axes directions, which may be obtained from the NMR data, are directly related to the atomic site symmetry and distortion. Similarly, we also expect the EPR fine structure constants D and E to be related to the deviations from perfect octahedral or tetrahedral symmetry also. (The Zeeman constants γ and g do not vary appreciably from one mineral to another, g being very close to the free electron value 2.00.)

For quantitative description of distortions from perfect octahedron or tetrahedron, it is necessary to define both the angular and the bond length deviations from ideal values for the coordination polyhedra. Robinson, Gibbs, and Ribbe (1971) have proposed the use of quadratic elongation as a measure for polyhedral distortion. Hamil (personal communication) has defined longitudinal strain $|\alpha|$ and shear strain $|\psi|$ for the coordination polyhedra:

$$|\alpha| = \sum_i |\ln (\ell_i/\ell_0)|, \quad (6)$$

$$|\psi| = \sum_i |\tan (\theta_i - \theta_0)|, \quad (7)$$

where ℓ_i is the individual Al–O bond length, ℓ_0 is the "ideal" bond length, a perfect polyhedron with bond length ℓ_0 having the same volume as the coordination polyhedra. θ_i is the individual O–Al–O

bond angle; θ_0 is the ideal bond angle, being 90° for octahedron and 109.5° for tetrahedron.

The longitudinal strain $|\alpha|$ is a measure of the variation of Al–O bond lengths, whereas the shear strain $|\psi|$ is a measure of the deviations of O–Al–O bond angles. We will follow the conventions of Hamil, since it is easier to distinguish between bond length and bond angle effects by using both $|\alpha|$ and $|\psi|$.

Discussion

Site assignment of ^{27}Al NMR spectra

Before we attempt a correlation between quadrupole coupling constant C for ^{27}Al with polyhedral distortion, we would like to discuss the problem of site assignment of the NMR spectra for structures with more than one crystallographically different Al-site. Andalusite, sillimanite, cordierite, and synthetic rare-earth aluminum garnets each have two crystallographically distinct Al-sites. The principal axes directions of the quadrupole coupling tensors may be used to distinguish between the two sites, in case the sites possess different point-group symmetries. In sillimanite, the octahedral and tetrahedral Al-sites have point group symmetries $\bar{1}$ and m respectively. Hence, the principal axes have no restriction for the octahedral site, while for the tetrahedral site one of the principal axes must be perpendicular to the mirror plane (Raymond and Hafner, 1970). In synthetic rare-earth aluminum garnets, the octahedral and tetrahedral Al-sites have point group symmetries $\bar{3}$ and $\bar{4}$ respectively. Hence, for the octahedral site one of the principal axes must be parallel to the $\bar{3}$ axis, while for the tetrahedral site, one of the principal axes must be parallel to the $\bar{4}$ axis (see, e.g., Tsang and Ghose, 1971). In these two cases, the site assignment of the NMR spectra is unambiguous. However, both andalusite and cordierite have two Al-sites, with point group symmetries 2 and m respectively, which cannot be distinguished by NMR spectra alone. In andalusite, one unusually large quadrupole coupling constant (15.6 MHz) can be assigned to the highly distorted octahedral Al-site (Hafner, Raymond, and Ghose, 1970). This assignment has been confirmed by calculation of the electric field gradient from a point charge model, taking the dipole and quadrupole moment of the oxygen ions into account (Raymond, 1971). In cordierite, Al^{3+} ions are ordered in tetrahedral T_1 and T_5 sites, the T_1 site being much more distorted from regular tetrahedral symmetry than T_5 (Gibbs, 1966). Ac-

cordingly, the larger quadrupole coupling constant has been assigned to the T_1 site, subsequently confirmed by a calculation of the electric field gradient from a point charge model (Tsang and Ghose, 1972b).

In anorthite, Al occurs in eight crystallographically different sites (Wainwright and Starkey, 1971). Brinkmann and Staehli (1968) have determined eight ^{27}Al quadrupole coupling tensors, but were unable to make any site assignments.

Tetrahedral Al-sites

In Table 1, the published NMR and EPR constants for tetrahedral AlO_4 sites are tabulated. The longitudinal strain $|\alpha|$ and shear strain $|\psi|$ for the AlO_4 tetrahedra are calculated from refined crystal structures. Correlation between nuclear quadrupole coupling constant C and longitudinal strain $|\alpha|$ is very poor whereas that between C and the shear strain $|\psi|$ is qualitatively good, and a roughly linear relationship may be obtained. Since, $|\alpha| \ll |\psi|$ for AlO_4 tetrahedra, it appears that C depends mostly on shear (angular) strain and only slightly on longitudinal strain.

If so, the largest and the smallest quadrupole coupling constants for anorthite may be tentatively assigned to the most and least distorted Al-sites, namely, T_1 ($0zi0$) and T_2 ($mzi0$). A more satisfactory method of site assignment of the NMR spectra in anorthite would be through comparison of the measured electric field gradients with those calculated based on the point charge model including the dipole and quadrupole moments of oxygen. So far, no such calculation has been attempted for anorthite.

Octahedral Al-site

In Table 2, some of the NMR and EPR results for octahedral AlO_6 sites have been tabulated along with the longitudinal $|\alpha|$ and shear strains $|\psi|$ from the refined crystal structures. The situation is, however, quite different from tetrahedrally coordinated Al sites. Table 2 shows that correlation between the nuclear quadrupole coupling constant C and $|\psi|$ is very poor, whereas that between C and $|\alpha|$ is fair. In general, a fairly good linear relationship between C and $|\alpha|$ exists (Fig. 1). There are, however, three anomalous data points (indicated by crosses in Figure 1): spodumene, corundum, and the Al_2 site (symmetry m) of chrysoberyl. Excluding these anomalous points, the root mean square deviation of the experimental points from the straight line is 1.2 MHz.

Previously, Hafner, Raymond, and Ghose (1970)

TABLE 1. Tetrahedrally Coordinated Sites (D in cm^{-1}, e^2qQ/h in MHz)

Mineral	Fe^{3+}		^{27}Al		Distortion		References
	D	$3E/D$	e^2qQ/h	η	$\lvert\alpha\rvert$	$\lvert\psi\rvert$	
Natrolite $Na_2Al_2Si_3O_{10}\cdot2H_2O$	$0.108^§$	0.48	$1.66^§$	0.50	.043	.135	(S) Meier 1960 (F) Abdulsabirov et al. 1967 (A) Petch & Pennington 1962
Sillimanite Al_2SiO_5	0.17	0.9	6.77	0.53	.068	.400	(S) Burnham 1963a (F) LeMarshall et al. 1971 (A) Raymond & Hafner 1970
Microcline $KAlSi_3O_8$	$0.106^†$	1.0	$3.22^†$	0.21	.033	.336	(S) Finney & Bailey 1964 (F) Marfunin et al. 1967 (A) Hafner & Hartmann 1964
Albite $NaAlSi_3O_8$	$0.180^†$	0.20	$3.29^†$	0.62	.015	.427	(S) Ribbe et al. 1969 (F) Marfunin et al. 1967 (A) Hafner & Hartmann 1964
Cordierite $Mg_2Al_4Si_5O_{18}\cdot\eta H_2O$ T_1-site	$1.36^†$	0.58	$10.6^†$	0.38	.094	1.082	(S) Gibbs 1966 (F) Hedgecock et al. 1966 (A) Tsang & Ghose 1972b
Cordierite T_5-site			5.6	0.34	.058	.284	(S) Gibbs 1966 (A) Tsang & Ghose 1972b
Petalite $LiAlSi_4O_{10}$	0.24	0.02			.034	.757	(S) Liebau 1961 (F) Ja 1970
Gd, Al-garnet $Gd_3Al_5O_{12}$ (Note 1)			5.47	0^*	.023	.636	(S) Euler & Bruce 1965 (A) Tsang & Ghose 1971
Y, Al-garnet $Y_3Al_5O_{12}$ (Note 1)	$0.103^†$	0^*	$6.02^†$	0^*	.023	.636	(S) Euler & Bruce 1965 (F) Rimai & Kushida 1966 (A) Brog et al. 1966
Berlinite $AlPO_4$			4.09	0.37	.015	.21	(S) Schwartzenbach 1966 (A) Brun et al. 1961a
Anorthite $CaAl_3Si_2O_8$							(S) Wainwright & Starkey 1971 (A) Brinkmann & Staehli 1968
T1(0z00)					.060	.693	
T1(0zi0)			8.42	0.66	.058	.847	
T1(m000)					.065	.411	
T1(m0i0)					.056	.409	
T2(0000)					.053	.309	
T2(00i0)					.040	.648	
T2(mz00)					.037	.372	
T2(mzi0)			2.66	0.66	.049	.246	
			7.25	0.76			
			6.81	0.65			
			6.30	0.88			
			5.44	0.42			
			4.90	0.75			
			4.32	0.53			
Average			5.76		.052	.492	

* *Axial site symmetry requires $\eta = 0$ and $E = 0$.*
† *Good agreement between NMR ^{27}Al and EPR Fe^{3+} principal axes.*
§ *Poor agreement between NMR ^{27}Al and EPR Fe^{3+} principal axes.*
(S) *Structural data*   (F) *Fe^{3+} EPR data*   (A) *^{27}Al NMR data.*

pointed out that the nuclear quadrupole coupling constant C for octahedrally coordinated ^{27}Al may be related to the parameter Δ, the difference between largest and smallest Al–O distances of the coordination polyhedron. Their idea is consistent with our conclusion that C for AlO_6 depends on bond length variations.

Correlation of ^{27}Al Quadrupole Coupling Constant C *with the Crystal Field Parameter* D *of* Fe^{3+} *Replacing* Al^{3+} *in Aluminosilicates*

The crystal field parameter D in the spin Hamil-

tonian is also a measure of the departure of the crystal field from spherical symmetry. Since the crystal radii of Al^{3+} and Fe^{3+}, 0.50 and 0.64 Å (Pauling, 1960), are similar and the electronic charge distribution in the Fe^{3+} ion ($^6S_{5/2}$) is spherically symmetric, replacement of Al^{3+} by Fe^{3+} in the structure should not cause large distortion. Hence, a correlation between D for Fe^{3+} and C for ^{27}Al is expected. Burns (1961) measured the temperature dependence of quadrupole coupling constants for ^{27}Al in ferroelectric $C(NH_2)_3 Al(SO_4)_2 \cdot 6H_2O$ and for Ga in its Ga analog. He also measured the temperature de-

S. GHOSE, AND T. TSANG

TABLE 2. Octahedrally Coordinated Sites (D in cm^{-1}, e^2qQ/h in MHz)

Mineral	Fe^{3+} D	$3E/D$	^{27}Al e^2qQ/h	η	Distortion $|\alpha|$	$|\psi|$	References
Corundum $\alpha\text{-}Al_2O_3$	0.17[†]	0*	2.39[†]	0*	0.172	1.511	(S) Newnham & de Haan 1962 (F) Bogle & Symmons 1959 (A) Pound 1950
Beryl $Be_3Al_2(SiO_3)_6$	0.017[†]	0*	3.09[†]	0*	0.062	1.445	(S) Gibbs et al. 1968 (F) Dvir & Low 1960 (A) Brown & Williams 1956
Euclase $HBeAlSiO_5$			5.17	0.70	0.126	1.047	(S) Mrose & Appleman 1962 (A) Eades 1955
Sillimanite Al_2SiO_5	1.18	0.34	8.93	0.46	.118	.803	(S) Burnham 1963a (F) Le Marshall et al. 1971 (A) Raymond & Hafner 1970
Chrysoberyl $BeAl_2O_4$ $Al_1(\bar{1})$			2.85	0.94	.074	1.269	(S) Farrell et al. 1963 (F) Vinokurov et al. 1962 (A) Hockenberry et al. 1958
Chrysoberyl $Al_2(m)$	0.20	0.05	2.85	0.76	.166	1.037	
Spodumene $LiAl(SiO_3)_2$	0.13[§]	0.19	2.95[§]	0.94	.226	1.089	(S) Clark et al. 1969 (F) Manoogian et al. 1965 (A) Petch et al. 1953
Kyanite Al_2SiO_5 Al_1	1.3	0.13	10.04	0.27	.149	1.134	(S) Burnham 1963b (F) Troup & Hutton 1964 (A) Hafner & Raymond 1967
Kyanite Al_2			3.70	0.89	.063	1.143	
Kyanite Al_3			6.53	0.59	.107	1.295	
Kyanite Al_4			9.37	0.38	.160	1.058	
Andalusite Al_2SiO_5 Al_1	1.88[†]	0	15.6[†]	0.08	.300	.632	(S) Burnham & Buerger 1961 (F) Holuj et al. 1966 (A) Hafner, Raymond & Ghose 1970
Andalusite Al_2 (5-coordinated)	1.40[†]	0.33	5.9[†]	0.70	not applicable		
Spinel $MgAl_2O_4$		0.25[†]	0*	3.68[†]	0*	.028	1.198	(S) Bacon 1952 (F) Brun et al. 1961b (A) Brun & Hafner 1962
Gahnite $ZnAl_2O_4$		0.34[†]	0*	3.68[†]	0	.016	.902	(S) Saalfeld 1964 (F) Drumheller et al. 1964 (A) Brun, Ghose & Schindler 1964
Gd, Al-garnet $Gd_3Al_5O_{12}$				< 0.1	0*	.008	.650	(S) Euler & Bruce 1965 (A) Tsang & Ghose 1971
Y, Al-garnet $Y_3Al_5O_{12}$		0.105[†]	0*	0.63[†]	0*	.008	.650	(S) Euler & Bruce 1965 (F) Rimai & Kushida 1966 (A) Brog et al. 1966
Grossular $Ca_3Al_2(SiO_4)_3$				3.61	0*	.002	.272	(S) Prandl 1966 (A) Derighetti & Ghose 1969
Almandine garnet $(Fe,Mg)_3Al_2(SiO_4)_3$				1.51	0*	.003	.356	(S) Zemann & Zemann 1961 (A) Ghose 1964
Zoisite $Ca_2Al_3Si_3O_{12}OH$ $Al_{1,2}$				8.05	0.46	.134	.741	(S) Dollase 1968 (F) Hutton et al. 1971 (A) Brinkmann, Staehli and Ghose 1969
Zoisite Al_3		0.79[†]	0.06	18.50[†]	0.16	.353	1.139	
Epidote $Ca_2Al_2(Fe,Al)Si_3O_{13}H$ Al_1				9.8	0.2	.161	.692	(S) Dollase 1971 (A) Tsang & Ghose (to be published)
Epidote Al_2				4.6	0.34	.073	.546	
Topaz $Al_2SiO_4F_2$		0.32[†]		1.67[†]	0.38	not applicable		(S) Ribbe & Gibbs 1971 (F) Thyer et al. 1967 (A) Tsang & Ghose 1972a

* *Axial site symmetry requires* $\eta = 0$ *and* $E = 0$.
† *Good agreement between NMR* ^{27}Al *and EPR* Fe^{3+} *principal axes.*
§ *Poor agreement between NMR* ^{27}Al *and EPR* Fe^{3+} *principal axes.*
(S) *Structural data*   (F) Fe^{3+} *EPR data*   (A) ^{27}Al *NMR data.*

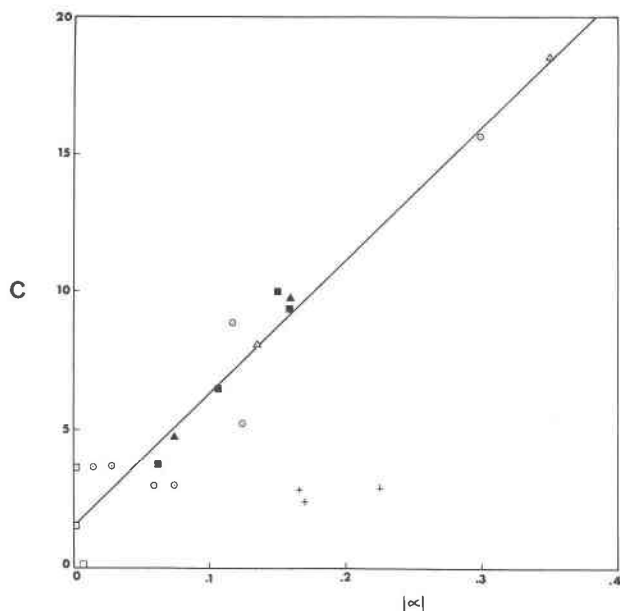FIG. 1. Nuclear quadrupole coupling constant C in MHz vs $|\alpha|$ for octahedrally coordinated ^{27}Al. Open triangles, zoisite (left, $Al_{1,2}$; right, Al_3). Filled triangles, epidote (left, Al_2; right, Al_1). Open squares, garnets (top to bottom, grossular, almandine garnet, $Gd_3Al_5O_{12}$). Filled squares, kyanite (left to right, Al_2, Al_3, Al_1, Al_4). Crosses, left to right: Al_2-site of chrysoberyl, corundum, spodumene. Circles, left to right: gahnite, spinel ($MgAl_2O_4$), beryl, Al_1-site of chrysoberyl, sillimanite, euclase, andalusite.

pendence of the EPR spectra of Cr^{3+} replacing Al^{3+} or Ga^{3+}. By parametrically eliminating temperature, the plots of D vs C give two parallel but displaced lines, one for the two sites in the two Al compounds and the other for the two Ga compounds. From theoretical considerations, Burns (1961) presented a relation between D and C as:

$$D = -\frac{3}{112}\left(\frac{\Delta g}{g_f}\right)^2 \frac{\langle r^2 \rangle h}{(1 - \gamma_\infty)Q}(e^2 Qq/h) \quad (8)$$

where $\Delta g = g - g_f$ and $\langle r^n \rangle$ is the expectation value of r^n over the $3d$ electron wave function.

The measurements show that although D and $e^2 Qq/h$ are linearly related, $D \neq 0$ when $q = 0$ and the slope of the curve is an order of magnitude larger than the calculated value. The reason for this disagreement is not clear.

In aluminosilicates the correlation between C and D for both octahedrally and tetrahedrally coordinated sites is poor (Tables 1, 2). Furthermore, correlation between η and $3E/D$ and the agreements between NMR and EPR principal axes systems are also

quite unpredictable, except in andalusite (Hafner, Raymond, and Ghose, 1970).

This lack of correlation means that the replacement of Al^{3+} by trace amounts of Fe^{3+} in the aluminosilicate structure usually causes a distortion of the surrounding oxygen coordination polyhedra in an unpredictable manner. Careful X-ray diffraction studies of pure Al_2O_3 and Fe^{3+}-bearing Al_2O_3 crystals indicate that Fe^{3+} ions are shifted about 0.06Å as compared with Al^{3+}, and the shift is opposite to the calculated direction (Moss and Newnham, 1964). There are few detailed studies of substitutional effects of Al^{3+} by Fe^{3+}. Further research is urgently needed, since the steric details of Al^{3+} and Fe^{3+} coordination polyhedra may differ more than is commonly realized.

Conclusions

1. The ^{27}Al nuclear quadrupole coupling constants are correlated with the distortions of nearest-neighbor oxygen coordinations from ideal polyhedra.

a. For AlO_4 tetrahedra, the quadrupole coupling constant C depends mostly on shear strain and slightly on longitudinal strain. Hence, bond angle variations are more important than bond length variations.

b. For AlO_6 octahedra, on the other hand, the quadrupole coupling constant depends mostly on longitudinal strain and hence bond length variations are more important.

2. There is usually no correlation between the ^{27}Al quadrupole coupling constant and the zero field splitting parameter D for Fe^{3+} (trace amounts) replacing Al^{3+} in aluminosilicates.

This probably means that Fe^{3+} replacement distorts the Al–O site considerably in aluminosilicate structures.

References

ABDULSABIROV, R. Y., V. M. VINOKUROV, M. M. ZARIPOV, AND V. G. STEPANOV (1967) Electron paramagnetic resonance of Fe^{3+} ions in natrolite. *Sov. Phys. Solid State,* **9,** 541–542.

ABRAGAM, A., AND B. BLEANEY (1970) *Electron Paramagnetic Resonance of Transition Ions.* Oxford University Press, New York.

BACON, G. E. (1952) A neutron diffraction study of magnesium aluminum oxide. *Acta Crystallogr.* **5**, 684–686.

BOGLE, G. S., AND H. Y. SYMMONS (1959) Paramagnetic resonance of Fe^{3+} in sapphire at low temperatures. *Proc. Phys. Soc. (London)*, **73**, 531–532.

BRINKMANN, D., AND J. L. STAEHLI (1968) Magnetische Kernresonanz von ^{27}Al in Anorthit, $CaAl_2Si_2O_8$. *Helv. Phys. Acta*, **41**, 274–281.

BRINKMANN, D., J. L. STAEHLI, AND S. GHOSE (1969) Nuclear magnetic resonance of ^{27}Al and ^1H in zoisite. *J. Chem. Phys.* **51**, 5128–5133.

BROG, K. C., W. H. JONES, AND C. M. VERBER (1966) ^{27}Al and ^{89}Y nuclear magnetic resonance in Y-Al garnet. *Phys. Lett. (Netherlands)*, **20**, 258–260.

BROWN, L. C., AND D. WILLIAMS (1956) Quadrupolar splitting of ^{27}Al and ^9Be magnetic resonances in beryl crystals. *J. Chem. Phys.* **24**, 751–756.

BRUN, E., AND S. S. HAFNER (1962) Die elektrische Quadrupolaufspaltung von Al^{27} in Spinell $MgAl_2O_4$ und Korund Al_2O_3. *Z. Kristallogr.* **117**, 37–62.

———, S. GHOSE, AND P. SCHINDLER (1964) ^{27}Al nuclear magnetic resonance in zinc spinels. *Helv. Phys. Acta,* **37**, 626.

———, P. HARTMANN, F. LAVES, AND D. SCHWARTZENBACH (1961a) Elektrische Quadrupolwechselwirkung von Al^{27} in $AlPO_4$. *Helv. Phys. Acta,* **34**, 388–391.

———, H. LOELIGER, AND F. WALDNER (1961b) Paramagnetische Elektronenresonanz von Fe^{3+} in einem natürlichen $MgAl_2O_4$ Spinell. *Bull. Ampère,* **10**, 167–169.

BURNHAM, C. W. (1963a) Refinement of the crystal structure of sillimanite. *Z. Kristallogr.* **118**, 127–148.

——— (1963b) Refinement of the crystal structure of kyanite. *Z. Kristallogr.* **118**, 337–360.

———, AND M. J. BUERGER (1961) Refinement of the crystal structure of andalusite. *Z. Kristallogr.* **115**, 269–290.

BURNS, G. (1961) Nuclear quadrupole resonance and electron spin resonance in $C(NH_2)_3Al(SO_4)_2 \cdot 6H_2O$ and isomorphous compounds. *Phys. Rev.* **123**, 1634–1644.

CLARK, J. R., D. E. APPLEMAN, AND J. J. PAPIKE (1969) Crystal chemical characterization of clinopyroxenes based on eight new structure refinements. *Mineral. Soc. Amer. Spec. Pap.* **2**, 31–50.

COHEN, M. H., AND F. REIF (1957) Nuclear quadrupole resonance in solids. *Solid State Phys.* **5**, 321–443.

DERIGHETTI, B., AND S. GHOSE (1969) Nuclear magnetic resonance of ^{27}Al in the garnet grossularite. *Phys. Lett. (Netherlands)*, **28A**, 523–524.

DOLLASE, W. A. (1968) Refinement and comparison of the structures of zoisite and clinozoisite. *Amer. Mineral.* **53**, 1882–1898.

——— (1971) Refinement of the crystal structures of epidote, allanite, and hancockite. *Amer. Mineral.* **56**, 447–464.

DRUMHELLER, J. E., K. LOCHER, AND F. WALDNER (1964) Electron paramagnetic resonance of Cr^{3+} and Fe^{3+} in synthetic $ZnAl_2O_4$ spinel. *Helv. Phys. Acta,* **37**, 626–627.

DVIR, M., AND W. LOW (1960) Paramagnetic resonance and optical spectrum of iron in beryl. *Phys. Rev.* **119**, 1587–1591.

EADES, R. G. (1955) An investigation of the nuclear resonance absorption spectrum of Al^{27} in a single crystal of euclase. *Can. J. Phys.* **33**, 286–297.

EDMONDS, D. T., AND A. J. LINDOP (1968) Quadrupole splittings and paramagnetic shifts in NMR of ^{27}Al in rare earth aluminum garnets. *J. Appl. Phys.* **39**, 1008.

EULER, F., AND J. A. BRUCE (1965) Oxygen coordinates of of compounds with garnet structure. *Acta Crystallogr.* **19**, 971–978.

FARRELL, E. F., J. H. FANG, AND R. E. NEWNHAM (1963) Refinement of chrysoberyl structure. *Amer. Mineral.* **48**, 804–810.

FINNEY, J. J., AND S. W. BAILEY (1964) Crystal structure of an authigenic maximum microcline. *Z. Kristallogr.* **119**, 413–426.

GHOSE, S. (1964) Nuclear magnetic resonance spectrum of ^{27}Al in a natural almandine garnet $(Fe, Mg)_3Al_2(SiO_4)_3$. *Solid State Comm.* **2**, 361–362.

GIBBS, G. V. (1966) Polymorphism of cordierite. I. The crystal structure of low cordierite. *Amer. Mineral.* **51**, 1068–1087.

———, D. W. BRECK, AND E. P. MEAGHER (1968) Structural refinement of hydrous and anhydrous synthetic beryl and emerald. *Lithos,* **1**, 275–285.

HAFNER, S. S., AND P. HARTMANN (1964) Elektrischer Feldgradient und Sauerstoff-polarisierbarkeit in Alkali-Feldspaten, $NaAlSi_3O_8$ und $KAlSi_3O_8$. *Helv. Phys. Acta,* **37**, 348–360.

———, AND M. RAYMOND (1967) Nuclear quadrupole coupling tensors of Al^{27} in kyanite. *Amer. Mineral.* **52**, 1632–1642.

———, ———, AND S. GHOSE (1970) Nuclear quadrupole coupling tensors of ^{27}Al in andulusite Al_2SiO_5. *J. Chem. Phys.* **52**, 6037–6041.

HEDGECOCK, N. E., AND S. C. CHAKRAVARTY (1966) Electron spin resonance of Fe^{3+} in cordierite. *Can. J. Phys.* **44**, 2749–2756.

HOCKENBERRY, J. H., L. C. BROWN, AND D. WILLIAMS (1958) Nuclear resonance spectrum of ^{27}Al in chrysoberyl. *J. Chem. Phys.* **28**, 367–372.

HOLUJ, F., J. R. THYER, AND N. E. HEDGECOCK (1966) ESR spectra of Fe^{3+} in single crystals of andalusite. *Can. J. Phys.* **44**, 509–523.

HUTTON, D. R., G. J. TROUP, AND G. A. STEWART (1971) Paramagnetic ions in zoisite. *Science,* **1974**, 1259.

JA, Y. H. (1970) Electron paramagnetic resonance of Fe^{3+} and Mn^{2+} in natural single crystals of petalite. *Aust. J. Phys.* **23**, 299–310.

LE MARSHALL, J., D. R. HUTTON, G. J. TROUP, AND J. R. W. THYER (1971) A paramagnetic resonance study of Cr^{3+} and Fe^{3+} in sillimanite. *Phys. Stat. Solidi,* **A5**, 769–773.

LIEBAU, F. (1961) Zur Kristallstruktur von Petalit. *Acta Crystallogr.* **14**, 399–406.

LOW, W., AND E. L. OFFENBACHER (1965) Electron spin resonance of magnetic ions in complex oxides. *Solid State Phys.* **17**, 135–216.

MANOOGIAN, A., F. HOLUJ, AND J. W. CARSWELL (1965) Electron spin resonance of Fe^{3+} in single crystals of spodumene. *Can. J. Phys.* **43**, 2262–2275.

MARFUNIN, A. S., L. V. BERSHOV, M. L. MEILMANN, AND J. MICHOULIER (1967) Paramagnetic resonance of Fe^{3+} in some feldspars. *Schweiz. Mineral. Petrogr. Mitt.* **47**, 13–20.

MEIER, W. M. (1960) The crystal structure of natrolite. *Z. Kristallogr.* **113**, 430–444.

MOSS, S. C., AND R. E. NEWNHAM (1964) The chromium position in ruby. *Z. Kristallogr.* **120**, 359–363.

MROSE, M. E., AND D. E. APPLEMAN (1962) The crystal structures and crystal chemistry of väyrynenite (Mn, Fe)Be(PO₄)OH and euclase AlBeSiO₄OH. *Z. Kristallogr.* **117**, 16–36.

NEWNHAM, R. E., AND Y. M. DE HAAN (1962) Refinement of the α Al_2O_3, Ti_2O_3, V_2O_3 and Cr_2O_3 structures. *Z. Kristallogr.* **117**, 235–237.

PAULING, L. (1960) *The Nature of Chemical Bond.* Third edition, Cornell University Press, Ithaca, New York.

PETCH, H. E., N. G. CRANNA, AND G. M. VOLKOFF (1953) Second order nuclear quadrupole effects in single crystals. Part II. Experimental results for spodumene. *Can. J. Phys.* **31**, 837–858.

——, AND K. S. PENNINGTON (1962) Nuclear quadrupole coupling tensors for ^{23}Na and ^{27}Al in natrolite, a fibrous zeolite. *J. Chem. Phys.* **36**, 1216–1221.

POUND, R. V. (1950) Nuclear electric quadrupole interaction in crystals. *Phys. Rev.* **79**, 685–702.

PRANDL, W. (1966) Verfeinerung der Kristallstruktur des Grossulars mit Neutronen und Roentgenstrahlbeugung. *Z. Kristallogr.* **123**, 81–116.

RAYMOND, M. (1971) Electric field gradient calculations in the aluminosilicates (Al_2SiO_5). *Phys. Rev. B,* **3**, 3692–3702.

——, AND S. S. HAFNER (1970) Nuclear quadrupolar coupling tensors of ^{27}Al in silimanite, Al_2SiO_5. *J. Chem. Phys.* **53**, 4110–4111.

RIBBE, P. H., AND G. V. GIBBS (1971) The crystal structure of topaz and its relations to physical properties. *Amer. Mineral.* **56**, 24–30.

——, H. D. MEGAW, W. H. TAYLOR, R. B. FERGUSON, AND R. J. TRAILL (1969) The albite structures. *Acta Crystallogr.* **B25**, 1503–1518.

RIMAI, L., AND T. KUSHIDA (1966) Paramagnetic resonance of Fe^{3+} in YAl, LuAl and LuGa garnets. *Phys. Rev.* **143**, 160–164.

ROBINSON, K., G. V. GIBBS, AND P. H. RIBBE (1971) Quadratic elongation, a quantitative measure of distortion in coordination polyhedra. *Science,* **172**, 567–570.

SAALFELD, H. (1964) Strukturdaten von Gahnit $ZnAl_2O_4$. *Z. Kristallogr.* **120**, 476–478.

SCHMIDT, V. H., AND E. D. JONES (1970) Nuclear magnetic resonance study of thulium aluminum garnet. *Phys. Rev.* **B1**, 1978–1986.

SCHWARZENBACH, D. (1966) Verfeinerung der Struktur der Tiefquarz-modifikation von $AlPO_4$. *Z. Kristallogr.* **123**, 161–185.

THYER, J. R., S. M. QUICK, AND F. HOLUJ (1967) ESR spectrum of Fe^{3+} in topaz. *Can. J. Phys.* **45**, 3597–3610.

TROUP, G. J., AND D. R. HUTTON (1964) Paramagnetic resonance of Fe^{3+} in kyanite. *Brit. J. Appl. Phys.* **15**, 1493–1499.

TSANG, T., AND S. GHOSE (1971) Nuclear magnetic resonance of ^{27}Al in erbium and gadolinium aluminum garnets. *Phys. Stat. Solidi,* **B48**, K117–K120.

——, AND —— (1972a) Nuclear magnetic resonance ^{27}Al in topaz, $Al_2SiO_4(F, OH)_2$. *J. Chem. Phys.* **56**, 261–262.

——, AND —— (1972b) Nuclear magnetic resonance of ^1H and ^{27}Al and Al–Si order in low cordierite, $Mg_2Al_4Si_5O_{18} \cdot nH_2O$. *J. Chem. Phys.* **56**, 3329–3332.

VINOKUROV, V. M., M. M. ZARIPOV, V. G. STEPANOV, Y. E. POLSKII, G. K. CHERKIN, AND L. Y. SHEKUN (1962) Electron paramagnetic resonance in natural chrysoberyl. *Sov. Phys. Solid State,* **3**, 1797–1800.

WAINWRIGHT, J. E., AND J. STARKEY (1971) A refinement of the structure of anorthite. *Z. Kristallogr.* **133**, 75–84.

ZEMANN, A., AND J. ZEMANN (1961) Verfeinerung der Kristallstruktur von synthetischem Pyrop $Mg_3Al_2(SiO_4)_3$. *Acta Crystallogr.* **14**, 835–837.

ZUBKOVSKA, E., AND B. DERIGHETTI (1970) Kernresonanz von ^{27}Al in $Gd_3Al_5O_{12}$. *Helv. Phys. Acta,* **43**, 495.